ARTICLE

Manganese(II) bromo- and iodo-complexes with phosphoramidate and phosphonate ligands: synthesis, characterization and photoluminescence

Received 00th January 20xx,
Accepted 00th January 20xx

DOI: 10.1039/x0xx00000x

Marco Bortoluzzi,*[a,b] Jesús Castro,*[c] Andrea Di Vera,[a] Alberto Palù [a] and Valentina Ferraro [a]

Tetrahedral Mn(II) bromo- and iodo-complexes with phosphoramidate and phosphonate ligands were synthesized and characterized. Mononuclear complexes with general formula $[MnX_2L_2]$ were isolated by using the monodentate ligands $O=P(OPh)_2(NMe_2)$ and $O=P(OPh)_2Ph$. The bidentate resorcinol derivative 1,3-$O=P(NMe_2)O$-C_6H_4-$O(NMe_2)_2P=O$ behaved as bridging ligand, affording by reaction with MnX_2 salts a dinuclear complex in the case of X = Br and a coordination polymer for X = I, as revealed by single crystal X-ray diffraction. All the compounds showed the characteristic green photoluminescence of Mn(II) in tetrahedral environment. The lifetime values resulted influenced by the symmetry of the compounds. The complexes with $O=P(OPh)_2(NMe_2)$ in the coordination sphere showed high photoluminescence quantum yields.

1. Introduction

The chemistry of Mn(II) luminescent complexes is noticeably growing in the last years, and it strictly connected with the use of O-donor ligands based on pentavalent phosphorus.[1-2] The first luminescent phosphine oxide complex reported, $[MnBr_2(O=PPh_3)_2]$, is still of current interest due to its triboluminescent and ferroelectric properties.[3-6] Intriguing advances were recently achieved with the use of polydentate phosphine oxides, bidentate in particular, that allowed the isolation of mono-, di- and polynuclear complexes with coordination numbers from four to six and emissions in the green or orange-red regions of the visible spectrum, depending upon the coordination geometry.[7] Some of the compounds showed properties such as luminescent vapochromism and thermochromism, triboluminescence, dual emission and excitation-dependent luminescence.[8-15] The enhancement of the $^4T_1(^4G)\rightarrow{}^6A_1(^6S)$ emission achieved with the chelating ligand 4,6-bis(diphenylphosphino)dibenzofuran dioxide (DBFDPO) allowed the successful application of the tetrahedral complex $[MnBr_2(BDFDPO)]$ as active material in OLEDs.[16]

Another family of Mn(II) luminescent complexes was recently isolated by formally replacing the phosphine oxides with phosphoramides, arylphosphonic diamides and related species in the coordination sphere.[17-21] As for the phosphine oxides, aromatic fragments bonded through a carbon or a nitrogen atom to the phosphorus atom can sensitize the luminescence of Mn(II) because of the light-harvesting behaviour and the possibility of ligand-to-metal energy transfer. Dual emission was observed by introducing the naphthyl substituent in the skeleton of the ligand.

The results provided in the literature point out the paramount importance of species containing the [O=P]-donor moiety for the preparation of Mn(II) luminescent coordination compounds. The possibility of electronic and steric tuning given by the organic ligands represents an important degree of freedom with respect to $[MnX_4]^{2-}$ salts, that are finding several applications in advanced technology.[22-28]

Two classes of pentavalent phosphorus derivatives not yet explored for the preparation of Mn(II) luminescent coordination compounds are phosphoramidates and phosphonates, both containing –OR substituents bonded to the phosphorus atom. In this paper we report the synthesis, characterization and photoluminescence of tetrahedral bromo- and iodo-complexes with the monodentate ligands $O=P(OPh)_2(NMe_2)$ and $O=P(OPh)_2Ph$ and the bidentate species 1,3-$O=P(NMe_2)O$-C_6H_4-$O(NMe_2)_2P=O$. The ligands here considered are depicted together with their acronyms in Chart 1 for clarity.

[a] *Dipartimento di Scienze Molecolari e Nanosistemi, Università Ca' Foscari Venezia, Via Torino 155, I-30170 Mestre (VE), Italy. E-mail: markos@unive.it*
[b] *Consorzio Interuniversitario Reattività Chimica e Catalisi (CIRCC), via Celso Ulpiani 27, 70126 Bari, Italy*
[c] *Departamento de Química Inorgánica, Universidade de Vigo, Facultade de Química, Edificio de Ciencias Experimentais, 36310 Vigo, Galicia, Spain. E-mail: jesusc@uvigo.es*

Electronic Supplementary Information (ESI) available: Crystal data and structure refinement for **$[MnX_2(OP^{NOO})_2]$** (X = Br, I), Table S1. Crystal data and structure refinement for **$[Mn_2Br_4(\mu\text{-}OP^{NNO\sim ONN}PO)_2]$** and **$[MnI_2(\mu\text{-}OP^{NNO\sim ONN}PO)]_n$**, Table S2. IR and NMR spectra of **$OP^{NNO\sim ONN}PO$**, Fig. S1-S3. IR spectra of **OP^{COO}** and **$[MnBr_2(OP^{COO})_2]$**, Fig. S4. Extended description of the X-ray structures and of the supramolecular network of the crystalline compounds, Fig. S5-S18, Tables S3-S4. DFT-optimized structure of **$[MnBr_2(OP^{COO})_2]$** and pictures of the compound under ambient and UV light, Fig. S19. Cartesian coordinates of the DFT-optimized structure of **$[MnBr_2(OP^{COO})_2]$**, Table S5. CCDC 2077265, 2077266, 2045025 and 2045026. For ESI and crystallographic data in CIF or other electronic format see DOI: 10.1039/x0xx00000x

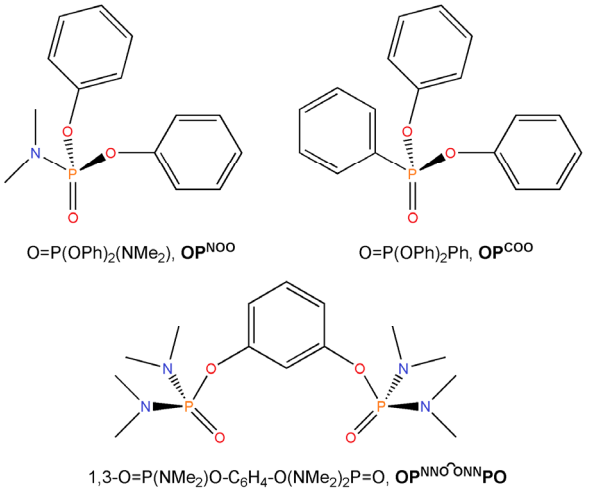

Chart 1 Phosphoramidates and phosphonate used in this work.

2. Experimental

2.1 Materials and methods

Commercial solvents (Merck) were purified as described in the literature.[29] Anhydrous Mn(II) halides were purchased from Alfa Aesar. The organic reactants were Merck products, used as received. $O=P(OPh)_2(NMe_2)$ (**OP^{NOO}**) and $O=P(OPh)_2Ph$ (**OP^{COO}**) were synthesized on the basis of reported procedures.[30-31] The syntheses of the Mn(II) complexes were carried out under inert atmosphere, working in a glove-box (MBraun Labstar with MB 10 G gas purifier) filled with N_2.

Elemental analyses (C, H, N) were carried out using an Elementar Unicube microanalyzer. Halide contents were determined using the Mohr's method.[32] Magnetic susceptibilities were measured on solid samples at 298 K with a MK1 magnetic susceptibility balance (Sherwood Scientific Ltd) and corrected for diamagnetic contribution by means of tabulated Pascal's constants.[33] Melting points were determined using a modified FALC 360 D instrument equipped with a camera. Conductivity measurements were carried out using a Radiometer Copenhagen CDM83 instrument. IR spectra were collected in the range 4000 – 400 cm^{-1} using a PerkinElmer Spectrum One spectrophotometer. Absorption spectra of dichloromethane solutions were collected in the range 235-700 nm with a Perkin-Elmer Lambda 35 spectrophotometer. Mono- and bidimensional nuclear magnetic resonance (NMR) spectra were collected at variable temperature with Bruker Avance 300 and Avance 400 instruments operating respectively at 300.13 MHz and 400.13 MHz of ^1H resonance. ^1H and ^{13}C $\{^1H\}$ NMR spectra are referred to the partially non-deuterated fraction of the solvent, itself referred to tetramethylsilane. ^{31}P $\{^1H\}$ NMR resonances are referred to 85% H_3PO_4 in water.

2.2 Synthesis of 1,3-O=P(NMe$_2$)O-C$_6$H$_4$-O(NMe$_2$)$_2$P=O, OP$^{NNO\frown ONN}$PO

A solution of 0.330 g (3.0 mmol) of 1,3-dihydroxybenzene (resorcinol) in 50 mL of EtOH was slowly added to a stirred solution of potassium *tert*-butoxide (0.673 g, 6.0 mmol) in 20 mL of EtOH. After 4 hours the solvent was evaporated under reduced pressure. In order to completely remove all the ethanol, about 10 mL of THF were added and the solvent was then evaporated again. The oil thus obtained was then dissolved in 50 mL of THF and *N*,*N*,*N*',*N*'-tetramethylphosphorodiamidic chloride (1.023 g, 6.0 mmol) was slowly added to the stirred solution. After 12 hours the cloudy reaction mixture was purified by centrifugation. The solvent was evaporated under reduced pressure and the resulting light brown oil was purified with toluene and isohexane. Yield = 70%.

2.2.1 Characterization of 1,3-O=P(NMe$_2$)O-C$_6$H$_4$-O(NMe$_2$)$_2$P=O. Anal. calcd for $C_{14}H_{28}N_4O_4P_2$ (378.24 g mol^{-1}, %): C, 44.44; H, 7.46; N, 14.81. Found (%): C, 44.25; H, 7.50; N, 14.74. ^1H NMR ($CDCl_3$, 298 K): δ 7.21 (t, 1H, J_{HH} = 8.1 Hz, Ar-H_5), 7.11 (s, 1H, Ar-H_2), 6.93 (d, 2H, J_{HH} = 8.1 Hz, Ar-H_4/H_6), 2.74 (d, 24H, J_{PH} = 10.0 Hz, NMe_2). ^{31}P $\{^1H\}$ NMR ($CDCl_3$, 298 K): δ 16.20 (FWHM = 4 Hz). ^{13}C $\{^1H\}$ NMR ($CDCl_3$, 298 K): δ 152.02 (d, J_{CP} = 6.2 Hz, Ar-C_1/C_3), 129.95 (Ar-C_5), 115.91 (d, J_{CP} = 5.2 Hz, Ar-C_4/C_6), 112.53 (t, J_{CP} = 5.0 Hz, Ar-C_2), 36.63 (d, J_{CP} = 4.2 Hz, NMe_2). IR (cm^{-1}): 3070-3000 m/w (aromatic ν_{C-H}), 2930-2820 m (ν_{C-H}), 1590-1490 m (aromatic ν_{C-C} and ν_{C-N}), 1320 m (ν_{C-O}), 1270-1160 s ($\nu_{P=O}$ and ν_{C-O}), 1133 s (ν_{C-N}), 1010 m (ν_{P-O}), 925 s (ν_{P-N}). UV-VIS (CH_2Cl_2, 298 K, nm): < 300, 266 (sh), 272 (max).

2.3 Synthesis of the complexes

The complexes were prepared by slowly adding a solution containing 2.1 mmol of $O=P(OPh)_2(NMe)$ or $O=P(OPh)_2Ph$ in 10 mL of EtOH to another solution of the proper anhydrous manganese salt MnX_2 (X = Br or I, 1.0 mmol) dissolved in 20 ml of EtOH. The reaction mixture was stirred overnight at room temperature under inert atmosphere. The solvent was then evaporated under reduced pressure and the solid was dissolved in the minimum amount of dichloromethane. The solution was cleared by centrifugation and the solvent was removed under reduced pressure. The solid products were separated by adding diethyl ether, filtered and dried *in vacuo*. The same procedure was applied for the preparation of the 1,3-O=P(NMe$_2$)O-C$_6$H$_4$-O(NMe$_2$)$_2$P=O complexes, using 1.1 mmol (0.416 g) of the bidentate phosphoramidate. Crystals suitable for X-Ray diffraction were collected from dichloromethane/diethyl ether or ethanol/dichloromethane/toluene solutions. Yield > 60% in all the cases.

2.3.1 Characterization of [MnBr$_2$(OP^{NOO})$_2$]. Anal. calcd for $C_{28}H_{32}Br_2MnN_2O_6P_2$ (769.26 g mol^{-1}, %): C, 43.72; H, 4.19; N, 3.64; Br, 20.77. Found (%): C, 43.54; H, 4.22; N, 3.60; Br, 20.85. M.p.: 125°C. χ^M_{corr} (c.g.s.u.): $1.42 \cdot 10^{-2}$. Λ_M (CH_2Cl_2, 298 K): < 2 $ohm^{-1}mol^{-1}cm^2$. IR (cm^{-1}): 1230-1150 s ($\nu_{P=O}$ and ν_{C-O}), 1010 m (ν_{P-O}), 950 s (ν_{P-N}).

2.3.2 Characterization of [MnI$_2$(OP^{NOO})$_2$]. Anal. calcd for $C_{28}H_{32}I_2MnN_2O_6P_2$ (863.26 g mol^{-1}, %): C, 38.96; H, 3.74; N, 3.25; I, 29.40. Found (%): C, 38.79; H, 3.75; N, 3.23; I, 29.52. M.p.: 107°C. χ^M_{corr} (c.g.s.u.): $1.54 \cdot 10^{-2}$. Λ_M (CH_2Cl_2, 298 K): < 2 $ohm^{-1}mol^{-1}cm^2$. IR (cm^{-1}): 1203-1120 s ($\nu_{P=O}$ and ν_{C-O}), 1030-930 s (ν_{P-O}, ν_{P-N}).

2.3.3 Characterization of [MnBr$_2$(OP^{COO})$_2$]. Anal. calcd for $C_{36}H_{30}Br_2MnO_6P_2$ (835.31 g mol^{-1}, %): C, 51.76; H, 3.62; Br, 19.13. Found (%): C, 51.55; H, 3.65; Br, 19.21. M.p.: 74°C. χ^M_{corr} (c.g.s.u.):

1.51·10^{-2}. Λ_M (CH_2Cl_2, 298 K): < 2 ohm^{-1}mol^{-1}cm^2. IR (cm^{-1}): 1236 s ($\nu_{P=O}$), 961 s (ν_{P-O}).

2.3.4 Characterization of [MnI$_2$(OP^{COO})$_2$]. Anal. calcd for $C_{36}H_{30}I_2MnO_6P_2$ (929.31 g mol^{-1}, %): C, 46.53; H, 3.25; I, 27.31. Found (%): C, 46.49; H, 3.19; I, 27.40. M.p.: 78°C. χ^M_{corr} (c.g.s.u.): 1.56·10^{-2}. Λ_M (CH_2Cl_2, 298 K): < 2 ohm^{-1}mol^{-1}cm^2. IR (cm^{-1}): 1224 s ($\nu_{P=O}$), 964 s (ν_{P-O}).

2.3.5 Characterization of [Mn$_2$Br$_4$(μ-OP$^{NNO\sim ONN}$PO)$_2$]. Anal. calcd for $C_{14}H_{28}Br_2MnN_4O_4P_2$ (593.09 g mol^{-1}, %): C, 28.35; H, 4.76; N, 9.45; Br, 26.94. Found (%): C, 28.25; H, 4.80; N, 9.39; Br, 27.05. M.p.: 167°C. χ^M_{corr} (c.g.s.u.): 1.47·10^{-2}. Λ_M (CH_2Cl_2, 298 K): < 2 ohm^{-1}mol^{-1}cm^2. IR (cm^{-1}): 1180-1130 s ($\nu_{P=O}$ and ν_{C-O}), 1010 m (ν_{P-O}), 980 s (ν_{P-N}).

2.3.6 Characterization of [MnI$_2$(μ-OP$^{NNO\sim ONN}$PO)]$_n$. Anal. calcd for $C_{14}H_{28}I_2MnN_4O_4P_2$ (687.09 g mol^{-1}, %): C, 24.47; H, 4.11; N, 8.15; I, 36.94. Found (%): C, 24.37; H, 4.09; N, 8.20; I, 37.00. M.p.: 167°C. χ^M_{corr} (c.g.s.u.): 1.49·10^{-2}. Λ_M (CH_2Cl_2, 298 K): < 2 ohm^{-1}mol^{-1}cm^2. IR (cm^{-1}): 1170-1120 s ($\nu_{P=O}$ and ν_{C-O}), 982 m (ν_{P-O}), 930 s (ν_{P-N}).

2.4 Crystal structures determinations

The crystallographic data were collected at CACTI (Universidade de Vigo) at 100 K (CryoStream 800) using a Bruker D8 Venture Photon 100 CMOS detector and Mo-Kα radiation (λ = 0.71073 Å) generated by a Incoatec high brilliance IμS microsource. The software APEX3[34] was used for collecting frames of data, indexing reflections, and the determination of lattice parameters, SAINT[34] for integration of the intensity of reflections, and SADABS[34] for scaling and empirical absorption correction. The crystallographic treatment was performed using the Oscail program,[35] and solved using the SHELXT program.[36] The structure was subsequently refined by a full-matrix least-squares based on F^2 using the SHELXL program.[37] Non-hydrogen atoms were refined with anisotropic displacement parameters. Hydrogen atoms were included in idealized positions and refined with isotropic displacement parameters. A non-merohedral twinning was found in the last stages of the refinement of **[Mn$_2$Br$_4$(μ-OP$^{NNO\sim ONN}$PO)$_2$]** and **[MnI$_2$(OP^{NOO})$_2$]** (β angle is between 103 and 104.5°) and was treated by using TwinRotMatr procedure in PLATON.[38] Further details concerning crystal data and structural refinement are given in Tables S1 and S2. CCDC CCDC 2077265, 2077266, 2045025 and 2045026 contain the supplementary crystallographic data for this paper.

2.5 Photoluminescence measurements

Measurements on solid samples were carried out using air-tight quartz sample holders, filled in glove-box to avoid interactions of the complexes with moisture. Photoluminescence emission (PL) and excitation (PLE) measurements were carried out at room temperature on solid samples by a Horiba Jobin Yvon Fluorolog-3 spectrofluorometer. A continuous-wave xenon arc lamp was used as source selecting the excitation wavelength by a double Czerny–Turner monochromator. A single grating monochromator coupled to a photomultiplier tube was used as detection system for optical emission measurements. Excitation and emission spectra were corrected for the instrumental functions. Time-resolved analyses were performed in multi channel scaling modality (MCS) by using pulsed UV led sources (Horiba SpectraLED, 265, 290 and 377 nm). The photoluminescence quantum yield (PLQY) of the Mn(II) complexes (solid state, r.t.) was measured by means of a OceanOptics HR4000CG UV-NIR detector, fiber-coupled to an integrating sphere connected to an OceanOptics LED source centred at 365 nm.

2.6 Computational details

The computational geometry optimizations of **[MnBr$_2$(OP^{COO})$_2$]**, sextet state, was carried out without symmetry constrains, using the range-separated hybrid functional ωB97X[39-41] and the def2 split-valence polarized basis set of Ahlrichs and Weigend.[42] The "unrestricted" formalism was applied and the absence of meaningful spin contamination was verified by comparing the computed $\langle S^2 \rangle$ value with the theoretical ones.[43] The software used was Gaussian 09.[44]

3. Results and Discussion

3.1 Synthesis and X-ray structure determinations

The monodentate phosphoramidate O=P(OPh)$_2$(NMe$_2$) (**OP^{NOO}**) was prepared by reacting diphenyl phosphoryl chloride with an excess of gaseous NHMe$_2$.[30] The phosphonate O=P(OPh)$_2$Ph (**OP^{COO}**) was obtained on the basis of a reported procedure, by reacting deprotonated phenol with dichlorophenylphosphine oxide.[31]

The bidentate species 1,3-O=P(NMe$_2$)O-C$_6$H$_4$-O(NMe$_2$)$_2$P=O (**OP$^{NNO\sim ONN}$PO**) was synthesized starting from resorcinol, deprotonated with potassium *tert*-butoxide and then reacted with *N*,*N*,*N*',*N*'-tetramethylphosphorodiamidic chloride. IR and NMR spectra are collected in ESI, Fig. S1-S3. The formation of a symmetrically functionalized resorcinol is indicated by the quite simple aromatic region of the ^{1}H NMR spectrum, composed by three resonances at 7.21 (triplet, 1H), 7.11 (singlet, 1H) and 6.93 (doublet, 2H) ppm. Four resonances, including *ipso*-C, are present in the high frequency region of the ^{13}C {^{1}H} NMR spectrum. The C$_2$ resonance at 112.53 ppm is a triplet with $^3J_{PC}$ coupling constant of 5.0 Hz, confirming the bond of the resorcinol fragment to two equivalent phosphorus atoms. The NMe$_2$ fragments are associated to a doublet at 2.74 ppm, with $^3J_{PH}$ coupling constant of 10.0 Hz. The related ^{13}C {^{1}H} NMR signal is a doublet at 36.63 ppm ($^2J_{PC}$ = 4.2 Hz).

The reaction of **OP^{NOO}** and **OP^{COO}** with anhydrous MnBr$_2$ and MnI$_2$ in ethanol afforded complexes having general formulae **[MnX$_2$(OP^{NOO})$_2$]** and **[MnX$_2$(OP^{COO})$_2$]**, as suggested by elemental analysis data and magnetic measurements, with magnetic moments close to the 5.9 BM expected for high spin d^5 metal complexes of the first transition series. The IR spectra showed bands roughly comparable to those of the free ligands, with slight variations attributable to the coordination to Mn(II), as already observed for similar compounds.[19-20] As an example, the IR spectra of **OP^{COO}** and **[MnBr$_2$(OP^{COO})$_2$]** are compared in Fig. S4.

In the case of the **OP^{NOO}** complexes the formation of compounds with coordination number four was ascertained by single crystal X-ray diffraction. Crystal data and structure refinements are collected in Table S1, while a representation of the two compounds is shown in Fig. 1.

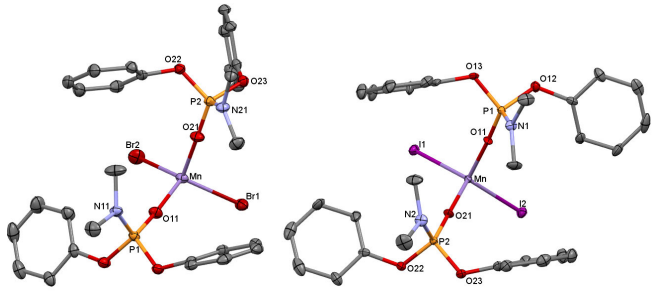

Fig. 1 X-ray structures of **[MnX$_2$(OP^{NOO})$_2$]** complexes.

The manganese ion is coordinated by two halide atoms and two oxygen atoms of the diphenyl dimethylphosphoramidate ligand. The most significant distances and angles are set out in Table 1.

Table 1 Selected bond lengths [Å] and angles [°] for **[MnX$_2$(OP^{NOO})$_2$]** complexes

	X=Br	X=I
Mn-X(1)	2.4479(4)	2.6788(9)
Mn-X(2)	2.4760(4)	2.6786(9)
Mn-O(11)	2.0416(14)	2.029(4)
Mn-O(21)	2.0525(14)	2.035(4)
P(1)-N(1)	1.6104(18)	1.623(5)
P(1)-O(11)	1.4755(14)	1.477(4)
P(1)-O(12)	1.5773(14)	1.580(4)
P(1)-O(13)	1.5692(14)	1.567(4)
P(2)-O(21)	1.4767(14)	1.474(4)
P(2)-O(22)	1.5721(14)	1.576(4)
P(2)-O(23)	1.5818(14)	1.572(4)
P(2)-N(2)	1.6102(17)	1.620(5)
X(1)-Mn-X(2)	117.168(14)	112.28(3)
O(11)-Mn-O(21)	97.90(6)	93.39(19)
O(11)-Mn-X(1)	112.74(4)	111.40(12)
O(11)-Mn-X(2)	108.86(4)	113.53(12)
O(21)-Mn-X(1)	105.40(4)	113.58(12)
O(21)-Mn-X(2)	113.12(4)	111.38(13)
P(1)-O(11)-Mn	176.14(10)	175.2(3)
P(2)-O(21)-Mn	164.73(10)	174.7(3)

The coordination polyhedron in the two complexes is best described as a slightly distorted tetrahedron, as expected for this kind of complexes.[19-21] In the ESI we describe in detail both the structures, but the different conformation of one of the ligands, evident in Fig. 1, produces some differences in the geometrical parameters. For example, on considering the angles around the Mn(II) centre, for **[MnBr$_2$(OP^{NOO})$_2$]** the Br-Mn-Br angle has the greatest value, 117.17(1)°, but in **[MnI$_2$(OP^{NOO})$_2$]** two of the I-Mn-O values are slightly greater than the I-Mn-I angle [113.58(12) and 113.53(12)° versus 112.28(3)° for I-Mn-I]. On the other hand, the O-Mn-O values are, as expected, more acute in the iodine compound [93.39(19) vs. 97.90(6)°], as well as the X-Mn-X angle. Another difference was found in the P-O-Mn angles, almost linear for both ligands in **[MnI$_2$(OP^{NOO})$_2$]** [av. 175°], but clearly bent in one of the ligands in **[MnBr$_2$(OP^{NOO})$_2$]**, 164.7(1)°, although far from the 145-150° range expected for [MnX$_2$(O=PR$_3$)$_2$] complexes.[18] All the other features are as expected for this kind of compounds. In particular, Mn-Br bond lengths are shorter than Mn-I ones, and longer Mn-O bonds correspond to shorter Mn-X interactions, so Mn-O bonds are larger in **[MnBr$_2$(OP^{NOO})$_2$]** by about 0.015 Å.

In the case of the bidentate phosphoramidate as ligand, characterization data of the isolated complexes were in agreement with a 1:1 stoichiometric ratio between **OP$^{NNO\sim ONN}$PO** and MnX$_2$ (X = Br, I). The κ^2 coordination mode was ruled out by means of single crystal X-ray diffraction, that revealed bridging coordination mode in both the isolated species, despite the fact that the two complexes are markedly different. In the case of X = Br the formula is **[Mn$_2$Br$_4$(μ-OP$^{NNO\sim ONN}$PO)$_2$]**, while a coordination polymer having formula **[MnI$_2$(μ-OP$^{NNO\sim ONN}$PO)]$_n$** was obtained for X = I. The two compounds are shown in Fig. 2. Crystal data and structure refinements are summarized in Table S2. Selected distances and angles are collected in Table 2.

Table 2 Selected bond lengths [Å] and angles [°] for **[Mn$_2$Br$_4$(μ-OP$^{NNO\sim ONN}$PO)$_2$]** and **[MnI$_2$(μ-OP$^{NNO\sim ONN}$PO)]$_n$**

	[Mn$_2$Br$_4$(μ-OP$^{NNO\sim ONN}$PO)$_2$]	**[MnI$_2$(μ-OP$^{NNO\sim ONN}$PO)]$_n$**
Mn-X(1)	2.4653(17)	2.6742(7)
Mn-X(2)	2.4597(18)	2.6489(7)
Mn-O(11)	2.047(7)	2.035(3)
Mn-O(22^{i})	2.053(7)	2.036(3)
P(1)-N(11)	1.614(9)	1.618(4)
P(1)-N(12)	1.643(9)	1.626(4)
P(1)-O(11)	1.479(8)	1.490(3)
P(1)-O(12)	1.596(7)	1.587(3)
P(2)-N(21)	1.601(11)	1.620(4)
P(2)-N(22)	1.605(9)	1.620(4)
P(2)-O(21)	1.590(7)	1.585(3)
P(2)-O(22)	1.486(7)	1.495(3)
X(1)-Mn-X(2)	119.66(7)	114.27(2)
O(11)-Mn-O(22^{i})	101.2(3)	99.42(13)
O(11)-Mn-X(1)	110.9(2)	110.52(9)
O(11)-Mn-X(2)	105.3(2)	107.30(9)
O(22^{i})-Mn-Br(1)	105.4(2)	111.71(9)
O(22^{i})-Mn-Br(2)	113.0(2)	112.50(9)
P(1)-O(11)-Mn	148.3(5)	143.4(2)
P(2)-O(22)-Mn^{ii}	138.5(5)	145.7(2)

Symm. Op.: For **[Mn$_2$Br$_4$(μ-OP$^{NNO\sim ONN}$PO)$_2$]**: i=ii, 2-x, 1-y, 1-z; for **[MnI$_2$(μ-OP$^{NNO\sim ONN}$PO)]$_n$**, O(22i) should be read as O(12i): i, 0.5-x, y-0.5, 1.5-z; ii, 0.5-x, y+0.5, 1.5-z.

In the dimeric **[Mn_2Br_4(μ-$OP^{NNO\sim ONN}PO)_2$]** the Mn(II) centre in the asymmetric unit is coordinated by two bromide ligands and by an oxygen atom of the phosphoramidate ligand. The tetrahedral coordination environment is completed by another oxygen atom of a symmetry generated molecule (see the footnote of Table 2 and Fig. 2). The other donor oxygen atom of the phosphoramidate ligand is bonded to the Mn(II) centre of the same symmetry generated unit in so that a dimeric ring-like structure is produced. Bond lengths and angles around the manganese ion are as expected, further details are reported in the ESI.

The asymmetric unit of the related iodide complex is almost superimposable, but small differences in the disposition of the atoms (due to a twist of the Mn-O bond, see ESI) imply that the supramolecular arrangement resulted to be a zig-zag polymer growing in the *y* axis. The distance between the nearest manganese ions is 8.8446(9) Å, and it is related to atoms in the same chain. The Mn---Mn distance is longer than that found in the dimeric bromide compound, 8.043(4) Å.

It is worth noting that the P-O-Mn angles are clearly bent, even more acute than the 145-150° range established for [$MnX_2(O=PR_3)_2$] complexes[18]. All the other features are as expected for this kind of compounds, and the Mn-X and Mn-O bonds follow the trends previously described for the **[$MnX_2(OP^{NOO})_2$]** complexes.

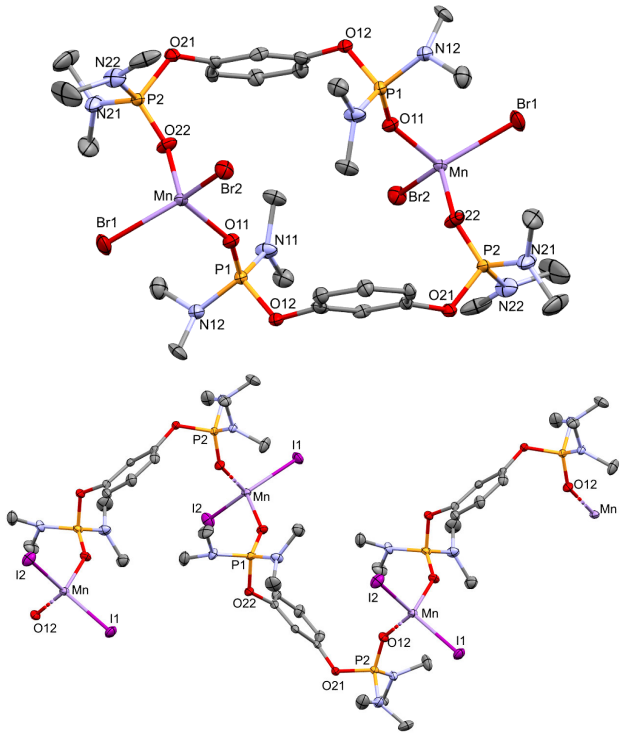

Fig. 2 X-ray structures of **[Mn_2Br_4(μ-$OP^{NNO\sim ONN}PO)_2$]** and **[MnI_2(μ-$OP^{NNO\sim ONN}PO$)]$_n$**.

3.2 Photoluminescence of the complexes

All the six compounds described are bright green photoluminescent upon excitation under UV light at the solid state, while no luminescence was detected in solution. The emission spectra of the **[$MnX_2(OP^{COO})_2$]** phosphonate complexes are comparable with those of the phosphoramidate derivatives and clearly support the tetrahedral coordination of Mn(II).[45-46] The DFT-optimized structure of **[$MnBr_2(OP^{COO})_2$]** is provided in ESI, Fig. S19, together with pictures of the complex under UV irradiation. The PL spectra of **[$MnX_2(OP^{NOO})_2$]**, **[$MnX_2(OP^{COO})_2$]**, **[Mn_2Br_4(μ-$OP^{NNO\sim ONN}PO)_2$]** and **[MnI_2(μ-$OP^{NNO\sim ONN}PO$)]$_n$** are shown in Fig. 3. Photoluminescence data are summarized in Table 3. No appreciable triboluminescence was observed for the six complexes.

The emissions are centred between 510 and 524 nm, with full width at half maximum (FWHM) values in the 2100 – 2700 cm^{-1} range. The related chromaticity coordinates fall in the green or yellowish green regions of the CIE 1931 chromaticity diagram.[47] In all the cases the photoluminescence is associated to the direct Mn(II) excitations $^4G \leftarrow {}^6A_1(^6S)$, between 400 and 490 nm, and $^4P,^4D \leftarrow {}^6A_1(^6S)$, between 330 and 390 nm. PLE bands are observable also for wavelengths below 300 nm, related to the $^4F \leftarrow {}^6A_1(^6S)$ transitions, superimposed to the excitation of the coordinated ligands. The inset of Fig. 3 shows as an example the PLE spectrum of **[$MnBr_2(OP^{NOO})_2$]**, where it is evident the separation of the ^4G manifold in three groups, $^4T_1$, $^4T_2$ and $^4A_1+{}^4E$. On the basis of the wavelength of the $(^4A_1+{}^4E)^4G \leftarrow {}^6A_1(^6S)$ transitions the Racah *B* parameter was estimated in the 720 – 735 cm^{-1} range for all the complexes. The value reported for the free ion is 923 cm^{-1},[48] therefore the nephelauxetic ratio β is around 0.79. Quite similar *B* and β parameters were reported for the coordination polymer $[Mn(NCN)]_n$, were Mn(II) is surrounded by an octahedral coordination sphere. In that case the Δ_o crystal filed splitting value was 8840 cm^{-1},[48] while the analysis of the d^5 Tanabe-Sugano diagram for the tetrahedral complexes here described afforded as expected lower values, with Δ_t crystal field spitting in the 3500 – 3750 cm^{-1} interval.

The lifetime values (τ) are all in the tenths of μs range, in line with other tetrahedral Mn(II) derivatives.[1] On comparing complexes with the same [O=P]-donor ligands in the coordination sphere, the reduction of the τ values on changing the halide from bromine to iodine is observable. Such a phenomenon is common for luminescent Mn(II) coordination compounds and it is explained on the basis of the acceleration of the radiative decay associated to the increased degree of spin–orbit coupling.[49] Comparable lifetimes were measured for **[$MnX_2(OP^{NOO})_2$]** and **[$MnX_2(OP^{COO})_2$]** complexes with the same halide, with τ values of the iodo-complexes about half with respect to the bromo-derivatives. On the other hand, the polynuclear compounds with the **$OP^{NNO\sim ONN}PO$** ligand showed markedly different τ values on changing the halide, as observable from the semi-log plots of the luminescence decay curves in Fig. 4. The τ value of the dinuclear species **[Mn_2Br_4(μ-$OP^{NNO\sim ONN}PO)_2$]** is 468 μs, while in this case of **[MnI_2(μ-$OP^{NNO\sim ONN}PO$)]$_n$** τ is about one order of magnitude lower, 40 μs. In both the compounds the Mn---Mn distances are longer than 8 Å, so interactions among Mn(II) centres can be ruled out. The lifetime difference can be tentatively explained on the basis of the different molecular structures. Differently from

the other complexes, **[$Mn_2Br_4(\mu$-$OP^{NNO\sim ONN}PO)_2$]** has approximate C_i symmetry (RMS = 0.0006), therefore it is roughly centrosymmetric. The computed dipole moment is 0.001 D, while for instance that of **[$MnBr_2(OP^{NOO})_2$]** is 15.332 D. It is likely to suppose that the centrosymmetry of **[$Mn_2Br_4(\mu$-$OP^{NNO\sim ONN}PO)_2$]** could reduce the probability of the $^4T_1(^4G)\rightarrow{}^6A_1(^6S)$ transition, causing the meaningful increase of the τ value with respect to the other compounds here reported.[50]

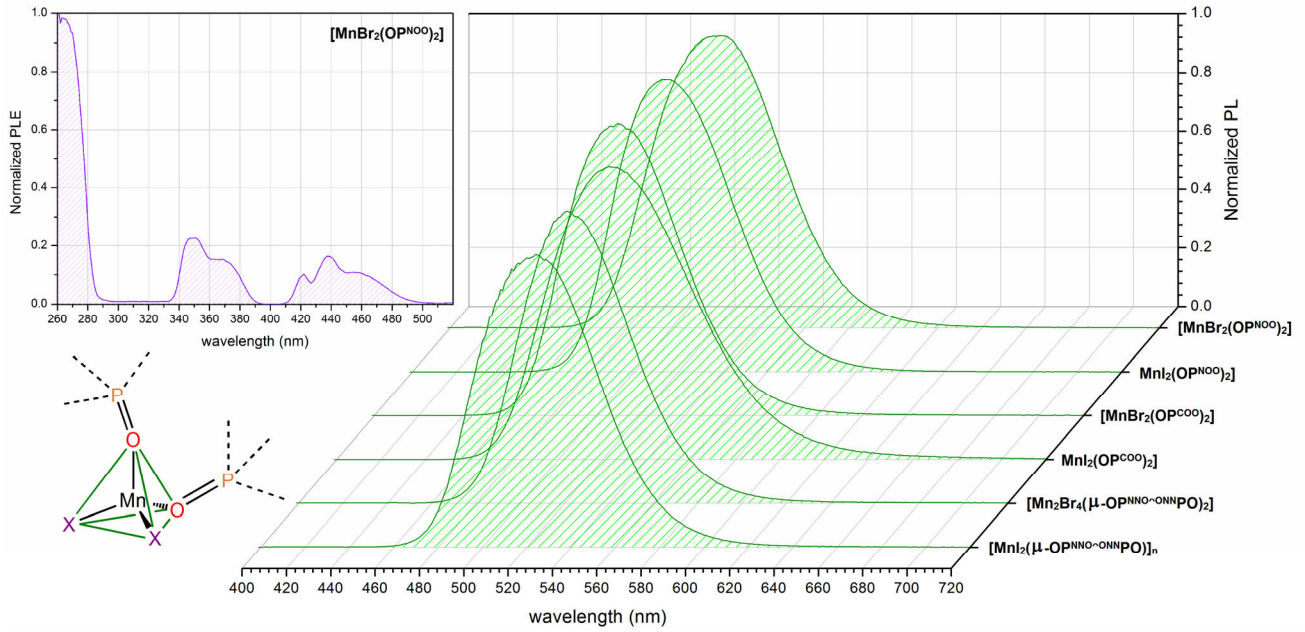

Fig. 3 Emission spectra of the Mn(II) complexes (green) and PLE spectrum of **[$MnBr_2(OP^{NOO})_2$]** (violet).

Table 3 Photoluminescence data of the complexes (solid samples, r.t.).

	PL, nm (FWHM, cm^{-1})	PLE, nm	CIE 1931	τ, μs	[a] Φ, %
[$MnBr_2(OP^{NOO})_2$]	[b] 520 $^4T_1(^4G)\rightarrow{}^6A_1(^6S)$, FWHM = 2500	[b] 458, 438, 421 $^4G\leftarrow{}^6A_1(^6S)$ 370, 349 $^4P,^4D\leftarrow{}^6A_1(^6S)$ < 290 $^4F\leftarrow{}^6A_1(^6S)$, ligands	x = 0.214 y = 0.664	[c] 173	58
[$MnI_2(OP^{NOO})_2$]	[d] 515 $^4T_1(^4G)\rightarrow{}^6A_1(^6S)$, FWHM = 2200	[d] 489-438, 426 $^4G\leftarrow{}^6A_1(^6S)$ 382, 370, 357, 348 $^4P,^4D\leftarrow{}^6A_1(^6S)$ < 305 $^4F\leftarrow{}^6A_1(^6S)$, ligands	x = 0.194 y = 0.660	[e] 93	84
[$MnBr_2(OP^{COO})_2$]	[f] 510 $^4T_1(^4G)\rightarrow{}^6A_1(^6S)$, FWHM = 2300	[f] 458, 438, 421 $^4G\leftarrow{}^6A_1(^6S)$ 370, 348 $^4P,^4D\leftarrow{}^6A_1(^6S)$ < 335 $^4F\leftarrow{}^6A_1(^6S)$, ligands	x = 0.168 y = 0.617	[g] 155	10
[$MnI_2(OP^{COO})_2$]	[h] 523 $^4T_1(^4G)\rightarrow{}^6A_1(^6S)$, FWHM = 2700	[h] 462, 444, 427 $^4G\leftarrow{}^6A_1(^6S)$ 379, 368, 358, 350 $^4P,^4D\leftarrow{}^6A_1(^6S)$ < 310 $^4F\leftarrow{}^6A_1(^6S)$, ligands	x = 0.278 y = 0.632	[h] 89	4
[$Mn_2Br_4(\mu$-$OP^{NNO\sim ONN}PO)_2$]	[d] 521 $^4T_1(^4G)\rightarrow{}^6A_1(^6S)$, FWHM = 2100	[d] 461, 440, 423 $^4G\leftarrow{}^6A_1(^6S)$ 372, 354, 346 $^4P,^4D\leftarrow{}^6A_1(^6S)$ < 300 $^4F\leftarrow{}^6A_1(^6S)$, ligands	x = 0.228 y = 0.679	[i] 468	17
[$MnI_2(\mu$-$OP^{NNO\sim ONN}PO)]_n$	[j] 524 $^4T_1(^4G)\rightarrow{}^6A_1(^6S)$, FWHM = 2300	466, 444, 427 $^4G\leftarrow{}^6A_1(^6S)$ 388-345 $^4P,^4D\leftarrow{}^6A_1(^6S)$; 282, 269, 262 $^4F\leftarrow{}^6A_1(^6S)$, ligands	x = 0.233 y = 0.668	[c] 40	15

[a] $\lambda_{excitation}$ = 365 nm. [b] $\lambda_{excitation}$ = 350 nm, $\lambda_{emission}$ = 560 nm. [c] $\lambda_{excitation}$ = 265 nm, $\lambda_{emission}$ = 520 nm. [d] $\lambda_{excitation}$ = 270 nm, $\lambda_{emission}$ = 560 nm. [e] $\lambda_{excitation}$ = 265 nm, $\lambda_{emission}$ = 515 nm. [f] $\lambda_{excitation}$ = 270 nm, $\lambda_{emission}$ = 515 nm. [g] $\lambda_{excitation}$ = 290 nm, $\lambda_{emission}$ = 510 nm. [h] $\lambda_{excitation}$ = 265 nm, $\lambda_{emission}$ = 523 nm. [i] $\lambda_{excitation}$ = 377 nm, $\lambda_{emission}$ = 522 nm. [j] $\lambda_{excitation}$ = 270 nm, $\lambda_{emission}$ = 550 nm.

An intriguing feature of the mononuclear **[$MnX_2(OP^{NOO})_2$]** complexes is related to the measured photoluminescence quantum yields (Φ). Values of 58% and 84% were obtained for **[$MnBr_2(OP^{NOO})_2$]** and **[$MnI_2(OP^{NOO})_2$]**, respectively. It is worth

noting that values exceeding 50% for Mn(II)-based green emitters are typical of $[MnX_4]^{2-}$ tetrahalides with suitable cations and neutral halide complexes with 4,6-bis(diphenylphosphino)dibenzofuran dioxide or bis[2-(diphenyl-phosphino)phenyl]ether dioxide in the coordination sphere.[1,8,16,51] The other compounds have Φ values comprised between 4% and 17%, in line with previous reports on comparable species.[17-20] The spectra used for the determination of the photoluminescence quantum yield of **$[MnI_2(OP^{NOO})_2]$** are shown as an example in Fig. 5.

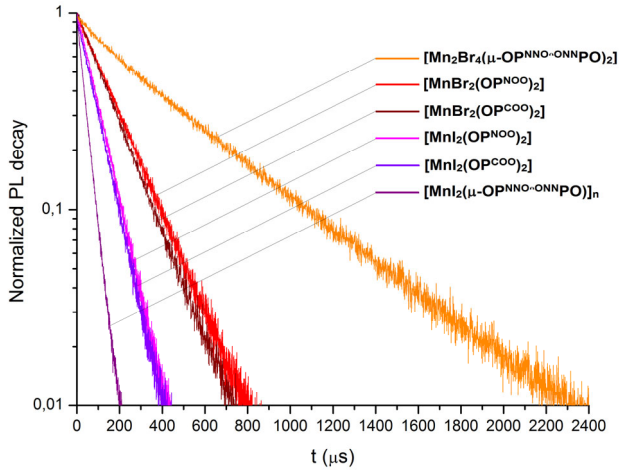

Fig. 4 Semi-log plots of the luminescence decay curves.

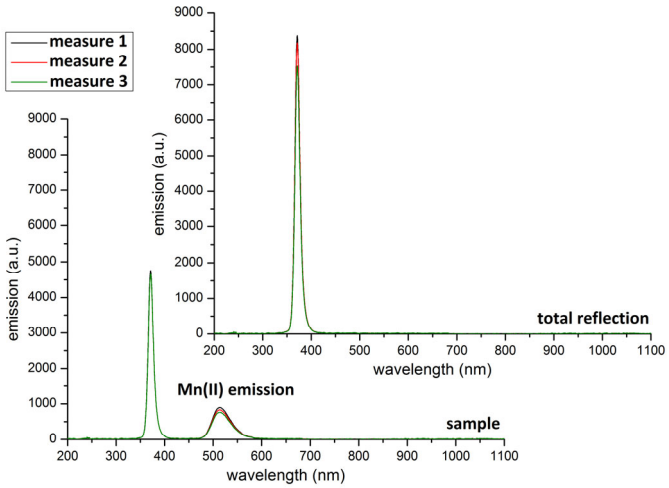

Fig. 5 Emission spectra used for the determination of **$[MnI_2(OP^{NOO})_2]$** photoluminescence quantum yield.

The high photoluminescence quantum yield values allow to conclude that the steric bulk and the rigidity of the coordinated **OP^{NOO}** ligands reduce the probability of non-radiative decays. Moreover, the lack of meaningful conjugation avoids metal→ligand energy transfers, possibly followed by vibrational relaxation. This last consideration is supported by the higher quantum yield of **$[MnI_2(OP^{NOO})_2]$** with respect to **$[MnBr_2(OP^{NOO})_2]$**. The similar coordination sphere and the quite low wavenumbers of the Mn–X vibrations suggest that the difference is not related to non-radiative decay in the first coordination sphere.[52] The shorter lifetime (see Table 3) probably makes less competitive back-energy transfer processes followed by ligand-centred vibrational relaxation.

Conclusions

The results provided in this paper indicate that phosphoramidate and phosphonate are suitable ligands for the preparation of Mn(II) complexes. The use of a bidentate phosphoramidate afforded a dinuclear complex and a coordination polymer, depending upon the choice of the MnX_2 precursor. In all the cases the typical green emission of Mn(II) in tetrahedral environment was observed, but the symmetry of the compounds and the substituents at the phosphorus atom revealed to deeply influence quantities such as the lifetime of the excited states and the photoluminescence quantum yields.

Author Contributions

Marco Bortoluzzi: conceptualization, formal analysis, funding acquisition, supervision, writing original draft. Jesús Castro: formal analysis, investigation, supervision, writing original draft. Andrea Di Vera: formal analysis, investigation, validation. Alberto Palù: investigation. Valentina Ferraro: formal analysis, investigation, validation.

Conflicts of interest

There are no conflicts to declare.

Acknowledgements

Università Ca' Foscari Venezia is gratefully acknowledged for financial support (Bando Spin 2018, D. R. 1065/2018 prot. 67416). CACTI (University of Vigo) is gratefully acknowledged for X-ray data collection.

Notes and references

1 Y. Qin, P. She, X. Huang, W. Huang and Q. Zhao, *Coord. Chem. Rev.*, 2020, **416**, 213331.
2 P. Tao, S.-J. Liu and W.-Y. Wong, *Adv. Opt. Mater.*, 2020, **8**, 2000985.
3 D. M. L. Goodgame and F. A. Cotton, *J. Chem. Soc.*, 1961, 3735-3741.
4 B. P. Chandra and B. Rao Kaza, *J. Lumin.*, 1982, **27**, 101-107.
5 F. A. Cotton, L. M. Daniels and P. Huang, *Inorg. Chem.*, 2001, **40**, 3576-3578.
6 Y.-Y. Tang, Z.-X. Wang, P.-F. Li, Y.-M. You, A. Stroppa and R.-G. Xiong, *Inorg. Chem. Front.*, 2017, **4**, 154-159.
7 A. V. Artem'ev, M. P. Davydova, A. S. Berezin, V. K. Brel, V. P. Morgalyuk, I. Yu. Bagryanskaya and D. G. Samsonenko, *Dalton Trans.*, 2019, **48**, 16448-16456.

8 J. Chen, Q. Zhang, F.-K. Zheng, Z.-F. Liu, S.-H. Wang, A.-Q. Wu and G.-C. Guo, *Dalton Trans.*, 2015, **44**, 3289-3294.
9 Y. Wu, X. Zhang, L.-J. Xu, M. Yang and Z.-N. Chen, *Inorg. Chem.*, 2018, **57**, 9175 -9181.
10 M. Bortoluzzi, J. Castro, E. Trave, D. Dallan and S. Favaretto, *Inorg. Chem. Commun.*, 2018, **90**, 105-107.
11 A. S. Berezin, D. G. Samsonenko, V. K. Brelc and A. V. Artem'ev, *Dalton Trans.*, 2018, 47, 7306-7315.
12 Y. Wu, X. Zhang, Y.-Q. Zhang, M. Yang and Z.-N. Chen, *Chem. Commun.*, 2018, **54**, 13961-13964.
13 A. S. Berezin, M. P. Davydova, I. Yu. Bagryanskaya, O. I. Artyushin, V. K. Brel and A. V. Artem'ev, *Inorg. Chem. Commun.*, 2019, **107**, 107473
14 M. P. Davydova, I. A. Bauer, V. K. Brel, M. I. Rakhmanova, I. Yu. Bagryanskaya and A. V. Artem'ev, *Eur. J. Inorg. Chem.*, 2020, 695-703.
15 A. V. Artem'ev, M. P. Davydova, A. S. Berezin, T. S. Sukhikh and D. G. Samsonenko, *Inorg. Chem. Front.*, 2021, in press.
16 Y. Y. Qin, P. Tao, L. Gao, P. F. She, S. J. Liu, X. L. Li, F. Y. Li, H. Wang, Q. Zhao, Y. Q. Miao and W. Huang, *Adv. Opt. Mater.*, 2019, **7**, 1801160.
17 M. Bortoluzzi, J. Castro, F. Enrichi, A. Vomiero, M. Busato, W. Huang, *Inorg. Chem. Commun.*, 2018, **92**, 145-150.
18 M. Bortoluzzi and J. Castro, *J. Coord. Chem.*, 2019, **72**, 309-327.
19 M. Bortoluzzi, J. Castro, A. Gobbo, V. Ferraro, L. Pietrobon and S. Antoniutti, *New J. Chem.*, 2020, **44**, 571-579.
20 M. Bortoluzzi, J. Castro, A. Gobbo, V. Ferraro and L. Pietrobon, *Dalton Trans.*, 2020, **49**, 7525-7534.
21 M. Bortoluzzi, V. Ferraro and J. Castro, *Dalton Trans.*, 2021, **50**, 3132-3136.
22 S. Balsamy, P. Natarajan, R. Vedalakshmi and S. Muralidharan, *Inorg. Chem.*, 2014, **53**, 6054-6059.
23 C. Jiang, N. Zhong, C. Luo, H. Lin, Y. Zhang, H. Peng and C.-G. Duan, *Chem. Commun.*, 2017, **53**, 5954-5957.
24 L.-J. Xu, C.-Z. Sun, H. Xiao, Y. Wu and Z.-N. Chen, *Adv. Mater.*, 2017, **29**, 1605739.
25 S. Chen, J. Gao, J. Chang, Y. Zhang and L. Feng, *Sens. Actuators, B*, 2019, **297**, 126701.
26 J. Zhao, T. Zhang, X.-Y. Dong, M.-E. Sun, C. Zhang, X. Li, Y. S. Zhao and S.-Q. Zang, *J. Am. Chem. Soc.*, 2019, **141**, 15755-15760.
27 L. Mao, P. Guo, S. Wang, A. K. Cheetham and R. Seshadri, *J. Am. Chem. Soc.*, 2020, **142**, 13582-13589.
28 L.-J. Xu, X. Lin, Q. He, M. Worku and B. Ma, *Nat. Commun.*, 2020, **11**, 4329.
29 W. L. F. Armarego and D. D. Perrin, *Purification of laboratory chemicals*, Butterworth-Heinemann, Oxford, 4th edn, 1996.
30 M. Bortoluzzi, A. Di Vera, L. Pietrobon and J. Castro, *J. Coord. Chem.*, 2021, in press
31 A. J. Kendall, C. A. Salazar, P. F. Martino and D. R. Tyler, *Organometallics*, 2014, **33**, 6171-6178.
32 D. J. Pietrzyk and C. W. Frank, *Analytical Chemistry*, Academic Press, New York, 2nd edn, 2012.
33 G. A. Bain and J. F. Berry, *J. Chem. Educ.*, 2008, **85**, 532-536.
34 *Bruker, APEX3, SMART, SAINT,* Bruker AXS Inc., Madison, Wisconsin, USA, 2015.
35 P. McArdle, K. Gilligan, D. Cunningham, R. Dark and M. Mahon, *CrystEngComm*, 2004, **6**, 303-309.
36 G. M. Sheldrick, *Acta Crystallogr., Sect. A: Found. Crystallogr.*, 2015, **71**, 3-8.
37 G. M. Sheldrick, *Acta Crystallogr., Sect. C: Struct. Chem.*, 2015, **71**, 3-8.
38 A. L. Spek, *Acta Crystallogr., Sect. D: Biol. Crystallogr.*, 2009, **65**, 148-155.
39 Y. Minenkov, Å. Singstad, G. Occhipinti and V. R. Jensen, *Dalton Trans.*, 2012, **41**, 5526-5541.
40 J.-D. Chai and M. Head-Gordon, *Phys. Chem. Chem. Phys.*, 2008, **10**, 6615-6620.
41 I. C. Gerber and J. G. Ángyán, *Chem. Phys. Lett.*, 2005, **415**, 100-105.
42 F. Weigend and R. Ahlrichs, *Phys. Chem. Chem. Phys.*, 2005, **7**, 3297-3305.
43 C. J. Cramer, *Essentials of Computational Chemistry*, Wiley, Chichester, 2nd edn, 2004.
44 M. J. Frisch, G. W. Trucks, H. B. Schlegel, G. E. Scuseria, M. A. Robb, J. R. Cheeseman, G. Scalmani, V. Barone, B. Mennucci, G. A. Petersson, H. Nakatsuji, M. Caricato, X. Li, H. P. Hratchian, A. F. Izmaylov, J. Bloino, G. Zheng, J. L. Sonnenberg, M. Hada, M. Ehara, K. Toyota, R. Fukuda, J. Hasegawa, M. Ishida, T. Nakajima, Y. Honda, O. Kitao, H. Nakai, T. Vreven, J. A. Montgomery Jr., J. E. Peralta, F. Ogliaro, M. Bearpark, J. J. Heyd, E. Brothers, K. N. Kudin, V. N. Staroverov, R. Kobayashi, J. Normand, K. Raghavachari, A. Rendell, J. C. Burant, S. S. Iyengar, J. Tomasi, M. Cossi, N. Rega, J. M. Millam, M. Klene, J. E. Knox, J. B. Cross, V. Bakken, C. Adamo, J. Jaramillo, R. Gomperts, R. E. Stratmann, O. Yazyev, A. J. Austin, R. Cammi, C. Pomelli, J. W. Ochterski, R. L. Martin, K. Morokuma, V. G. Zakrzewski, G. A. Voth, P. Salvador, J. J. Dannenberg, S. Dapprich, A. D. Daniels, Ö. Farkas, J. B. Foresman, J. V. Ortiz, J. Cioslowski and D. J. Fox, Gaussian 09, Revision C.01, Gaussian Inc., Wallingford, CT, 2010.
45 U. Lanver and G. Lehmann, *J. Lumin.*, 1978, **17**, 225-235.
46 A. Harriman, *Coord. Chem. Rev.*, 1979, **28**, 147-175.
47 E. F. Schubert, *Light-emitting Diodes*, Cambridge University Press, 2nd edn, 2006, pp. 292–300.
48 X. Liu, R. Dronskowski, R. Glaum and A. L. Tchougréeff, *Z. Anorg. Allg. Chem.* 2010, **636**, 343-348.
49 M. Wrighton and D. Ginley, *Chem. Phys.*, 1974, **4**, 295-299.
50 D. C. Harris and M. D. Bertolucci, *Symmetry and Spectroscopy*, Oxford University Press, New York, 1978.
51 A. S. Berezin, M. P. Davydova, D. G. Samsonenko, T. S. Sukhikh and A. V. Artem'ev, *J. Lumin.*, 2021, **236**, 118069.
52 H. G. M. Edwards, M. J. Ware and L. A. Woodward, *Chem. Commun.*, 1968, 540–541.